Proceedings of the ASME 2010 International Design Engineering Technical Conferences & Computers and Information in Engineering Conference
IDETC/CIE 2010
August 15-18, 2010, Montreal, Quebec, Canada

DETC2010-28978

KINEMATIC-, STATIC- AND WORKSPACE ANALYSIS OF A 6-P-U-S PARALLEL MANIPULATOR

Madusudanan Sathia Narayanan, Sourish Chakravarty, Hrishi Shah, Venkat N Krovi*
Automation, Robotics and Mechatronics Laboratory (ARMLAB)
Department of Mechanical & Aerospace Engineering
State University of New York at Buffalo
Buffalo, New York 14260.
Email: [ms329, sc267, hlshah, vkrovi]@buffalo.edu

ABSTRACT

This paper examines the symbolic kinematic modeling of a general 6-P-U-S (prismatic-universal-spherical) parallel kinematic manipulator (PKM). The base location of actuators has been previously shown to lead to: (i) reduction of the (motor) weight carried by the legs; (ii) elimination of the actuation transmission requirement (through intermediary joints as in the case of the Stewart-Gough platform); and (iii) most-importantly absorption of reaction-forces by the ground. We focus on using the symbolic equations to derive the conditions for type I and II singularities of this class of parallel manipulators. Based on these conditions, this system of equations is specialized to a specific configuration of the platform that has superior structural design and comparatively minimal singularities within its workspace. A series of studies were conducted to investigate the quality of workspace as well as estimate the actuation requirements for a unit payload carried over their workspace using the symbolic Jacobian model for this specialized configuration.

INTRODUCTION

A parallel manipulator typically consists of a moving platform and a fixed base that are connected together by several limbs. Because of the closed-loop architecture, not all of the joints can be independently actuated and usually the number of actuated joints is selected to be equal to the number of degrees of freedom of the manipulator [1]. Parallel manipulators for which the number of chains is strictly equal to the number of d.o.f. of the end-effector are called fully parallel kinematic manipulators FPKMs).

Architecturally, there are many choices for type of legs, joints and numbers of attached legs to the platform which can be significant factors for determining the workspace and actuation requirements. Considerable efforts have focused on enumerating and classifying various types of parallel architecture manipulators [2]. Further significant efforts have also been expended for dimensional optimization (see e.g. [3]) to enhance kinematic, kinetostatic and dynamic performance of such systems.

It is also considered advantageous to locate the actuations adjacent to the fixed base (rather than attaching it midway in an articulated leg like the traditional Stewart-Gough platform). Such architectures proved to be beneficial based on the following factors [4]: (1) absorption of major portion of reaction forces by the ground resulting in almost vibration-free operation with light-weight mobile components, (2) reduced effect of inertia due to the elimination of actuator's weight, (3) absence of interference of actuators and routing cables due to base location of actuators. Further, by selecting the base actuated joint to be prismatic, the proximal links are not subjected to the bending moments and the corresponding stresses. The resulting class of 6-DOF P-U-S (prismatic–universal–spherical, shortly referred to as 6-P-U-S hereafter) FPKMs is generally composed of six sliding actuators, six fixed length links and a mobile platform (as in Figure 1). The sliders active prismatics move along linear motion guides that are fixed on the ground and hence such systems are also referred to colloquially as "HexaSlides" or "HexaGlides". The links are of

*Corresponding author, Phone: (716)-645-1430, Fax: (716)-645-2883.

constant length and are connected to the sliders through universal joints (U). The axes of the prismatic joints along which the centers of the universal joints are being translated will be referred to as the rail axes. Finally, the links are connected to the mobile platform through spherical joints (S).

Hence, in this paper we wish to symbolically investigate a specialized 6-P-U-S type FPKM system and study its workspace characteristics. Figure 1 shows a schematic diagram of a generalized 6-P-U-S manipulator for which the system level kinematic model was developed to study its workspace and singularities. Using the statics equation for this system, the actuation requirements were also examined for carrying a unit-payload over their workspace assuming the near-zero platform velocities.

The rest of the paper is thus organized as follows: In Section 3, a brief overview of past research related to design-, workspace- and static analysis for such class of manipulators is given. The complete kinematic model and analytical derivations of the FPKM considered in this paper are presented in Section 4. The simulation studies and the corresponding results are discussed in successive sections followed by a summary and scope for future work in the final section.

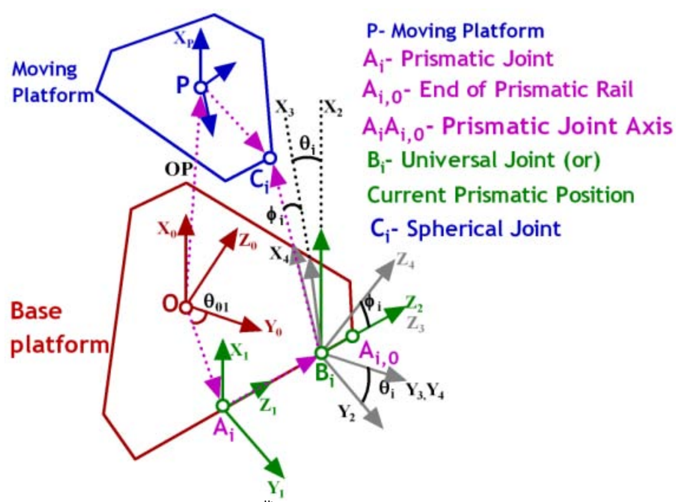

Figure 1: SCHEMATIC OF i^{th} LIMB OF 6-P-U-S HEXAPOD WITH REFERENCE FRAMES ATTACHED

LITERATURE REVIEW

Workspace and manipulability constitute important indexes for evaluating the performance of robot manipulators [5]. These were found to be sensitive especially for parallel manipulators as these have relatively small useful workspaces.

However, much of the earlier work related to kinematic- and workspace- analysis were primarily based on serial manipulators and simple parallel manipulators which can be found in [2, 6]. A detailed study of singularities and workspace analysis of parallel manipulator were discussed in [7]. Some of these were also based on studying the kinematics and workspace of parallel manipulators for a range of mechanisms [8]. Numerical workspace analyzes for Stewart platform were carried out in [9] and for other 6-DOF parallel platforms [10].

Numerical computation methods provided a starting point but tend to be limited by numerical errors. Moreover, always additional constraints need to be enforced in the algorithm to maintain the accuracy limits. Hence, developing closed-form analytical expressions for forward and inverse kinematics was realized as important. However, this proved to be a daunting task and has not been very successful for parallel architecture devices. Symbolic code-generation of kinematic and dynamic modeling was introduced that are capable of generating virtual prototypes based on standard approaches such as Lagrangian method [11-13].

There are also several known examples of 6-P-U-S systems— Hexaglide Robot (Figure 2.a) at ETH Zurich [14], the HexaM milling machine (Figure 2.b) by Toyoda [15], the active wrist (Figure 2.c) proposed in [16]. In [17], design of a 6-PSU platform (Figure 2.d) with 6 legs which had six vertical guides is discussed. Each leg comprises of a prismatic joint, spherical joint and universal joint that is used to connect the links to move the platform in six dimensional space.

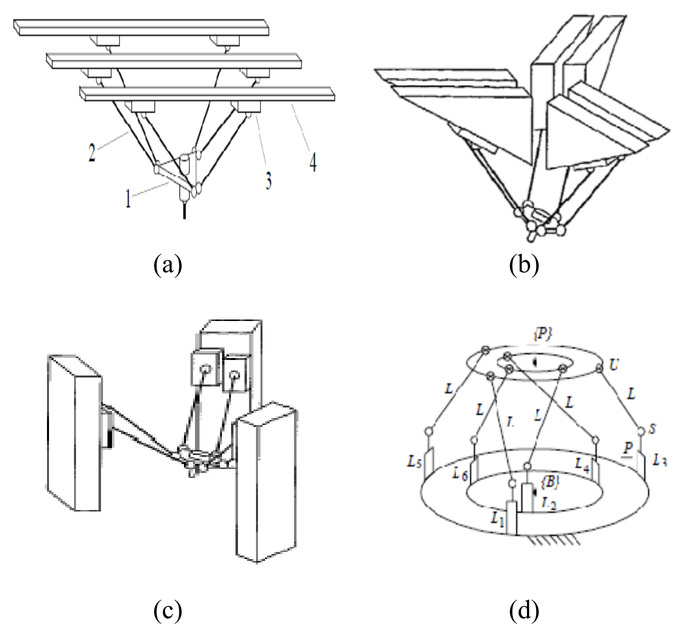

Figure 2: EXAMPLES OF 6-P-U-S PARALLEL MANIPULATORS (A) HEXAGLIDE ROBOT [14] (B) HEXA-M MILLING MACHINE [15] (C) ACTIVE WRIST [16] AND (D) 6-P-S-U PLATFORM [17]

The active wrist in (Figure 2.c) developed by Merlet and Gosselin, has the active prismatic joints move with respect to the base in which 3 pairs of prismatic sliders with fixed axes (all of them aligned vertically) drive 3 pairs of passive connecting links to move a distal platform. The 6 six prismatic joints for all cases (Figure 2) move with respect to the base and hence are not articulating. Closed form dynamics solutions were developed in [18-19] for a general 6-P-U-S manipulator.

However, it appears that the more fundamental kinematic analyses of workspace and singularity and its dependence on geometric parameters have not been considered systematically for a generalized case as well as a specialized case of 6-P-U-S manipulators. Hence, our focus is on using a symbolic approach to perform this analysis and examine singularities and workspace studies from this perspective. In this work, symbolically developing inverse kinematics and Jacobian were dealt with close attention, and its subsequent use to evaluate workspace performance and actuator requirements for a specific type of 6-P-U-S class of parallel manipulators were studied.

FORMULATION

System Definition

The platform manipulator considered in this paper, a 6-P-U-S manipulator, is similar in architecture to the one considered in [20]. A schematic diagram of the generalized manipulator is shown in Figure 1 and a detailed schematic for each limb subsystem for our specialized configuration is shown in Figure 3. The point ***O*** is the global origin of this system and a right handed base reference frame XYZ with center ***O*** is attached to the base. All other frames are defined with respect to this frame. The top platform is defined by the position of its center of mass, ***P*** and the 3D orientation of the plate in terms of Euler angles with respect to the global frame. The position of the platform is given by the cartesian coordinates, $(x,y,z)^T$ measured from the frame XYZ and the orientation angles (Euler angles about relative *x*-, *y*- and *z*- axes) are expressed as $(\alpha,\beta,\gamma)^T$. Rotation angles are defined as γ,β,α with respect to (w.r.t.) relative *Z*, *Y*, *X*- axes respectively in the same sequence and the matrix R_P^O that transforms rotation from platform ***P*** with reference to ***O*** and can be obtained as:

$$R_P^O = \begin{bmatrix} \cos\gamma\cos\beta & \cos\gamma\sin\beta\sin\alpha - \sin\gamma\cos\alpha & \cos\gamma\sin\beta\cos\alpha + \sin\gamma\sin\alpha \\ \sin\gamma\cos\beta & \sin\gamma\sin\beta\sin\alpha + \cos\gamma\cos\alpha & \sin\gamma\sin\beta\cos\alpha - \cos\gamma\sin\alpha \\ -\sin\beta & \cos\beta\sin\alpha & \cos\beta\cos\alpha \end{bmatrix} \quad (1)$$

The combined six dimensional vector representation of the position and orientation of the platform is defined as its pose, $\tilde{X} = [x \quad y \quad z \quad \alpha \quad \beta \quad \gamma]^T$.

The system has 6 limbs and in all the subsequent discussions, the subscript *i* indexes each limb, $\forall i = 1 \cdots 6$. The center of the spherical joint in i^{th} limb will be denoted by a platform attachment point, C_i and the corresponding base attachment points are indicated as A_i. The start and end points of the rails of the i^{th} prismatic joint are given by A_i and $A_{i,0}$ respectively. The point B_i indicates the current slider position which is also the center of universal joint of the i^{th} limb lying along $\overline{A_i A_{i,o}}$ (rail axis *i)*. The universal joint angles can be characterized in terms of θ_i and φ_i as in Figure 3.

The prismatic joints are considered as active joint coordinates (λ_i) of this manipulator that drives the top platform through the desired cartesian space trajectories. The distance between point A_i and B_i will be denoted by λ_i. Therefore, by manipulating the coordinates λ_i, the desired pose $(\tilde{X})$ of the platform, ***P*** can be achieved using the inverse kinematics mapping: $\tilde{X} = f(\lambda_1,\lambda_2,\lambda_3,\lambda_4,\lambda_5,\lambda_6)$.

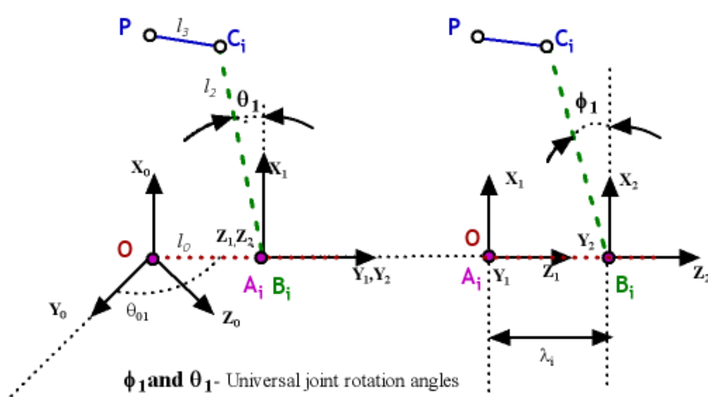

Figure 3: FRONT AND SIDE VIEW OF ITH LIMB OF 6-P-U-S MANIPULATOR

Position kinematics

For the position kinematics, the typical loop closure method [6] was used for an i^{th} limb of the 6-P-U-S platform to obtain vector equations similar to that of the Stewart Platform kinematic equations in [1].

$$\overrightarrow{OA_i} + \overrightarrow{A_iB_i} + \overrightarrow{B_iC_i} = \overrightarrow{OP} + \overrightarrow{PC_i} \quad (2)$$

The analytical procedure to solve Eqn. (2) for an inverse kinematic problem and to determine the joint coordinates of each limb, is already outlined in [20]. The solution of the resulting quadratic equation can, hence, be determined as:

$$\lambda_i = \hat{a}_i^T\left(\vec{d}_i\right) - \sqrt{\hat{a}_i^T\left(\vec{d}_i\right) - \vec{d}_i^T\left(\vec{d}_i\right) + \left(l_2\right)^2} \tag{3}$$

where, $\vec{d}_i$ is the leg vector as $\overrightarrow{B_iC_i}$, $\hat{a}_i$ be the unit vector along the rail axis slider $\overrightarrow{A_iB_i}$.

Velocity kinematics

Eqn. (2) is differentiated w.r.t. time as follows to obtain the velocity kinematics equation as follows:

$$\dot{\lambda}_i\,\hat{a}_i + \vec{\omega}_{B_iC_i} \times \overrightarrow{B_iC_i} = {}^{O}\!\left[\dot{\vec{p}}\right] + R_O^P \cdot {}^{P}\!\left[\vec{c}\right]$$

$$\overrightarrow{V_P} + \overrightarrow{\omega_P} \times {}^{O}\!\left[\overrightarrow{PC_i}\right] = \dot{\lambda}_i\,\hat{a}_i + \vec{\omega}_{B_iC_i} \times \overrightarrow{B_iC_i}, \quad \forall i = 1\cdots 6 \tag{4}$$

where, $\overrightarrow{V_P}$ is the translational velocity and $\overrightarrow{\omega_P}$ is the angular velocity vectors of the platform in 3D space. Dot-multiplying Eqn. (4) with $\overrightarrow{B_iC_i}$ on both sides to eliminate the passive leg angular velocity, $\vec{\omega}_{B_iC_i}$ terms and simplifying,

$$\left[\overrightarrow{B_iC_i} \quad {}^{O}\!\left(\overrightarrow{PC_i}\right) \times \overrightarrow{B_iC_i}\right] \begin{bmatrix} \vec{V}_P \\ \vec{\omega}_P \end{bmatrix} = \dot{\lambda}_i \left(\hat{a}_i \cdot \overrightarrow{B_iC_i}\right) \tag{5}$$

$$\forall i = 1\cdots 6$$

$$\Rightarrow \dot{\lambda}_i = \left(J_{link}\right)_i \begin{bmatrix} \vec{V}_P \\ \vec{\omega}_P \end{bmatrix}, \forall i = 1\cdots 6 \tag{6}$$

where, the link Jacobian matrix $\left(J_{link}\right)_i$ can be obtained as

$$\left(J_{link}\right)_i = \left[\left(J_q\right)_i\right]^{-1} \left(J_X\right)_i \tag{7}$$

where, $\left(J_X\right)_i = \left[\overrightarrow{B_iC_i} \quad {}^{O}\!\left(\overrightarrow{PC_i}\right) \times \overrightarrow{B_iC_i}\right]$ and $\left(J_q\right)_i = \hat{a}_i \cdot \overrightarrow{B_iC_i}$.

The link Jacobian matrix (Eqn. (7)) for the 6-P-U-S manipulator relates the prismatic joint velocity in the *i*th limb to the task space velocities of platform. Thus, by determining the Eqn. (6) for all the six limbs and cascading those into a single matrix will result in platform Jacobian matrix, J_P as:

$$J_P = \left(J_q\right)^{-1} J_X, \tag{8}$$

where,

$$J_q = \left[\hat{a}_1 \cdot \overrightarrow{B_1C_1} \quad \hat{a}_2 \cdot \overrightarrow{B_2C_2} \quad \hat{a}_3 \cdot \overrightarrow{B_3C_3} \cdots \cdots \hat{a}_4 \cdot \overrightarrow{B_4C_4} \quad \hat{a}_5 \cdot \overrightarrow{B_5C_5} \quad \hat{a}_6 \cdot \overrightarrow{B_6C_6}\right]_{6\times 6}$$

$$J_X = \begin{bmatrix} \overrightarrow{B_1C_1} & {}^{O}\!\left(\overrightarrow{PC_1}\right) \times \overrightarrow{B_1C_1} \\ \overrightarrow{B_2C_2} & {}^{O}\!\left(\overrightarrow{PC_2}\right) \times \overrightarrow{B_2C_2} \\ \vdots & \vdots \\ \overrightarrow{B_6C_6} & {}^{O}\!\left(\overrightarrow{PC_6}\right) \times \overrightarrow{B_6C_6} \end{bmatrix}_{6\times 6}$$

Specialization

The active prismatic joints of a generalized 6-P-U-S are located at any point and aligned along any direction in space. However, the location and orientation of the slider axis can be constrained to realize a design that would be structurally superior and mathematically easier to tackle compared to other designs discussed earlier. Specifically, it was aimed to modify the design that would lead to zero or minimal singular configurations. For this, a completely symbolic form of expressions for J_q and J_X was developed using Eqn. (8) to examine singularity conditions under which the Jacobian J_P of a generalized 6-P-U-S manipulator loses its full rank. It is already shown [7] that J_P can become singular only if J_q is singular (Type I singularity) or J_X is singular (Type II singularity) or both of them are singular (Type III singularity):

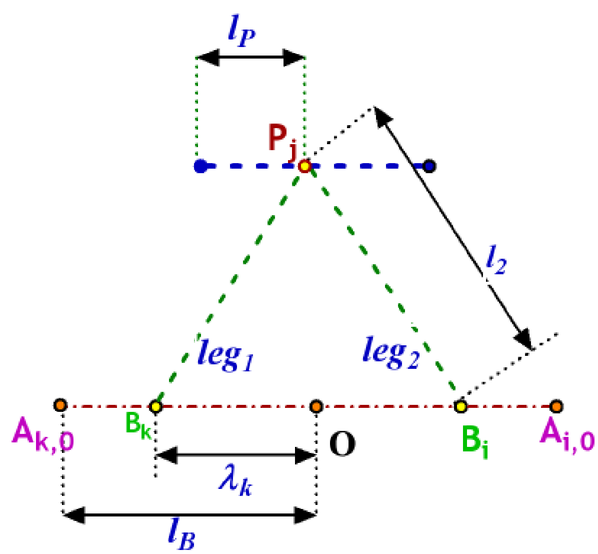

Figure 4: TWO-LEG SUBSYSTEM OF THE SPECIALIZED 6-P-U-S MANIPULATOR

Type I singularity. It gives rise to a set of singular configurations when the prismatic axes vector $\hat{a}_i$ becomes perpendicular to the leg vector $\overline{B_iC_i}$ for any one or more than one pair of a prismatic axis and the corresponding leg. Under this configuration, $\hat{a}_i \cdot \overline{B_iC_i} = 0$ should be true for one or more than one values of *i*.

It can thus be ensured by limiting the value of the universal joint within the range of +/- π/2 for both the joint axes' rotations that this manipulator is void of type I singularities within its workspace. It is also expected that enforcing such a constraint on the universal joint axes' rotations may only result in minimal reduction of the overall manipulator workspace.

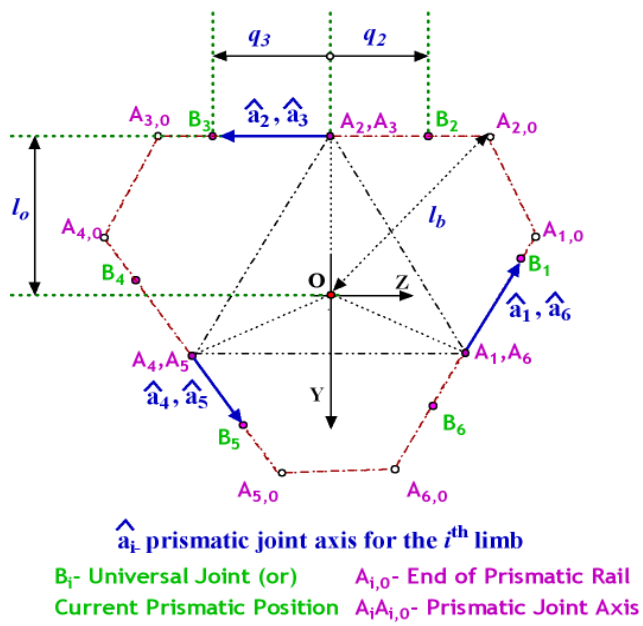

Figure 5: TOP VIEW OF 6-PUS MANIPULATOR AND ORIENTATION OF PRISMATIC JOINT AXES

Type II singularity. This can occur when J_X degenerates from the full rank (i.e.) when $\overline{B_iC_i}$ and $\overline{PC_i}$ are collinear or any row of J_X is linearly dependent on the other. However, by design the former situation will not occur under the complete set of operating conditions.

In order to design the manipulator with a superior structure different prismatic actuator alignments were considered and on analysis, the configuration as in Figure 6 was finalized. In order to enhance the structural stability and simplify the model further, it was assumed that a pair of legs attach to a common attachment point in the top platform. Thus, the specialized 6-P-U-S has three two-leg subsystems as in Figure 4 and Figure 7 connected together at three attachment points (C_j, $j=1,2,3$) in the top platform.

Suppose an arbitrary load (***F'***) acts on top of the platform resulting in action of a force, ***F*** along each leg on one of the three subsystems. The link vector $\overline{B_iC_i}$ will serve as a force only member as it is attached to the top platform by spherical and universal joints and will not transmit any moments.

Table 1: GEOMETRY OF THE 6-P-U-S		
Symbol	Values	Unit
Radius of prismatic origin L_o	0.1	m
Radius of base platform, L_b	0.125	m
Intermediate Link Length, L_2	0.120	m
Radius of top platform, L_P	0.080	m
Base attachment points (in frame ***O***)		
$A_{1,0}$ & $A_{6,0}$	[0, +/-0.1133, 0.0528]	m
$A_{2,0}$ & $A_{3,0}$	[0, +/-0.1024, 0.0717]	m
$A_{4,0}$ & $A_{5,0}$	[0,+/-0.0109, -0.1245]	m
Platform attachment points (in frame ***P***)		
C_1	[0.08, 0.0693, -0.04]	m
C_2	[0.08, 0.0, -0.08]	m
C_3	[0.08, -0.0693, -0.04]	m

Considering the free-body diagram in Figure 5, it can be observed that in each two-leg subsystem a major portion of the forces is transmitted to the ground. The symmetry of the structure will also cause the component of the forces along the slider axes within each two-leg subsystem to be largely counterbalanced (and thereby significantly reduce the actuation requirements). Thus, by carefully choosing the geometric and design parameters, a superior architecture for 6-P-U-S type manipulator was achieved. Further discussion on 6-P-U-S will be pertaining to this specialized configuration only.

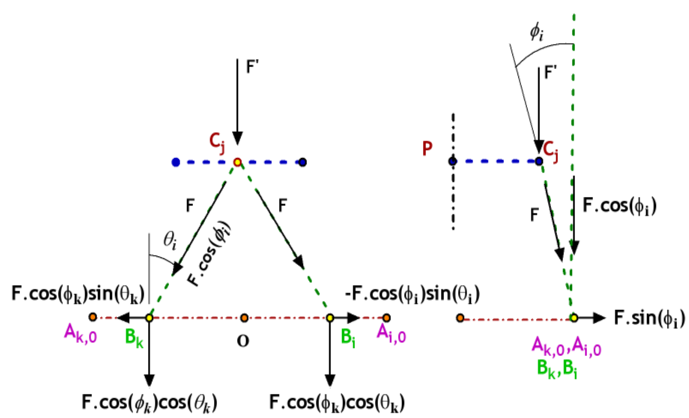

Figure 6: FREE BODY DIAGRAM FOR A TWO-LEG SUBSYSTEM OF A SPECIALIZED 6-P-U-S MANIPULATOR (INDICES *i and k ARE USED TO INDICATE THE POSITIONS OF A PAIR OF THE SLIDERS IN EACH SUBSYSTEM)*

This architecture is also advantageous in terms of computations required to solve the inverse kinematics. Since a pair of sliders can be defined using the same joint axes, $\hat{a}_i$ for this specialized configuration, there will be only three unique active joint axes as in Figure 6 and will result in simplified symmetric solutions for inverse kinematics. This will be evident from the joint trajectory plots in results sections. To augment our understanding of the geometry and workspace of this configuration, a detailed CAD model (using SolidWorks) and a physical prototype was also developed as shown in Figure **7**. The numerical values of the specialized 6-P-U-S are also available in the Table 1.

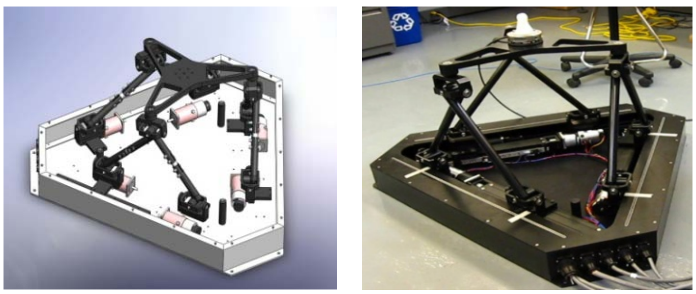

Figure 7: 3D CAD MODEL AND PHYISICAL PROTOTYPE OF 6-DOF P-U-S HEXAPOD SYSTEM

RESULTS

Workspace Envelopes- Translation and Orientation

For the specialized design of the manipulator system, the workspace envelopes were computed using inverse kinematics routine and discretizing the polar workspace region to search for the boundary points (the point at which the inverse kinematic equation (Eqn.(3)) fails to yield real solutions or fails to satisfy the actuator limits) along each radial directions from 0 to 2π radians. To obtain a more accurate estimate of the workspace envelopes, a finer discretized task space is desired. Finally, 2D workspaces were plotted for each value of the 3rd coordinate (the varying position or orientation coordinate) for a variety of cases. However, we show only for the two cases below:

(1) Zero orientation Translation Workspace (Figure 8)
(2) Zero Yaw-Pitch with Roll Orientation Workspace (Figure 9)

Workspace Analysis and Workspace Based Measures

While, by design this manipulator possesses minimal workspace singularities, the fluctuations in the quality of workspace using a range of Jacobian based measures (including Yoshikawa's measure, inverse condition number measure etc) were studied. The analytical Jacobian derived earlier facilitates performance of this workspace analysis and yields more accurate results than a numerical implementation.

Initially, the 3D-cartesian space was divided into 2D slices and each slice is then discretized into a sequence of uniformly spaced grid points spanning each 2D planes. The inverse kinematics was solved and analytical Jacobian was then evaluated at each of the grid points and the corresponding workspace measures were calculated. We show here only the Yoshikawa-measure (product of all the singular measures of the platform Jacobian matrix) to estimate the workspace quality of the specialized configuration (shown in Figure 10 and Figure 11). Since the visualization of 6-DOF workspace is not possible, only the constant orientation workspace of 6-P-U-S manipulator is presented here (for other types of workspace analysis refer [21]).

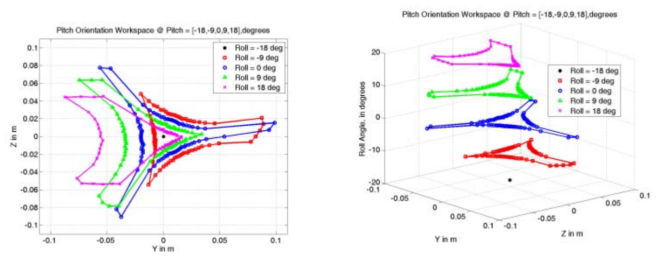

(A) (B)

Figure 8: ZERO-YAW-PITCH WORKSPACE LIMITS ON Y-Z PLANE FOR PITCH = -18, -9, 0, 9, 18 DEGREES (A) TOP VIEW (B) ISOMETRIC VIEW

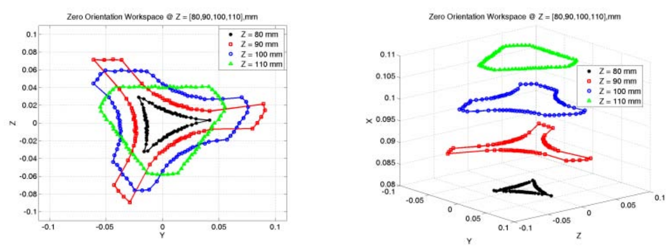

(A) (B)

Figure 9: ZERO ORIENTATION WORKSPACE LIMITS ON Y- Z PLANE FOR X = 0.080, 0.0900.100, 0.110 M (A) TOP VIEW (B) ISOMETRIC VIEW

Actuator Load Estimates by Static Analysis

In this section, the effect of Jacobian matrix on actuation requirements was studied by quasi-static analysis. The platform Jacobian matrix was used to compute the actuator forces for a known external load in task space assuming the platform is moving at near zero velocities. The quasi-static analysis was actually implemented by including the desired trajectory information into the formulation and computing actuator forces at each point in the trajectory. A subset of sample case studies are presented in Figure 12-14 for a constant vertical load of 1000 N along negative X-axis and zero loads and moments on all other directions for different trajectory tracking problems.

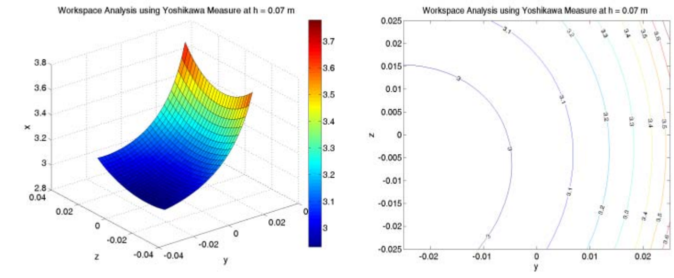

(A) (B)

FIGURE 10: CONSTANT ORIENTATION WORKSPACE MEASURE (A) SURFACE AND (B) CONTOUR PLOTS FOR X=0.070 α=0, β=0, γ=0; GRID: Y=Z=-0.025:0.025

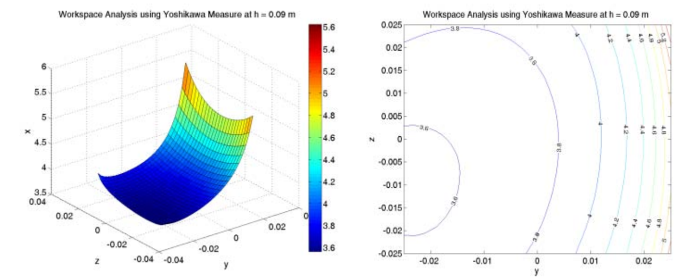

(A) (B)

FIGURE 11: CONSTANT ORIENTATION WORKSPACE MEASURE (A) SURFACE AND (B) CONTOUR PLOTS FOR X=0.090, α=0, β=0, γ=0; GRID: Y=Z=-0.025:0.025

Figure 12 indicates the static actuator load estimates for a vertical line trajectory. Similar results for the circular trajectory in YZ plane with radius = 0.01 m and yaw motion trajectory with an amplitude of 10 degrees are shown in Figure 13 and Figure 14 respectively.

CONCLUSION

In this paper, we wished to examine the workspace of 6-P-U-S that hitherto had not been done systematically. We developed symbolic equations for the inverse kinematics and the analytical Jacobian for the generalized 6-P-U-S manipulator. Using the symbolic elements, the manipulator architecture was specialized to the one that possesses minimal singularities within its workspace and has superior structural equilibration characteristics. We performed a series of kinematic and workspace analysis studies for this specialized architecture to further examine its feasibility and usability. Finally, we also performed a static analysis and provided an estimate of actuator forces for this specialized configuration for a set of desired trajectory problems.

An analytic workspace based design optimization is planned, building upon this detailed kinematic analysis. A complete inverse dynamic closed form solution for this specialized architecture is also planned to independently specify the actuator torques. This would in turn help us develop a model-based control scheme with enhanced performance of the manipulator.

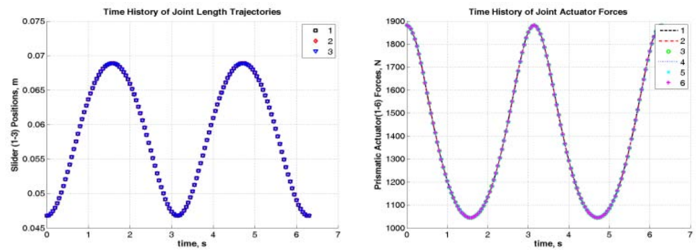

(A) (B)

Figure 12: ACTUATOR FORCE ESTIMATES FOR QUASI-STATIC SIMULATION FOR A STRAIGHT LINE TRAJECTORY X = 0.008*SIN(WT) M, Y=Z=0, ZERO ORIENTATION (A) ACTUATOR FORCES (B) ACTUATOR DISPLACEMENTS

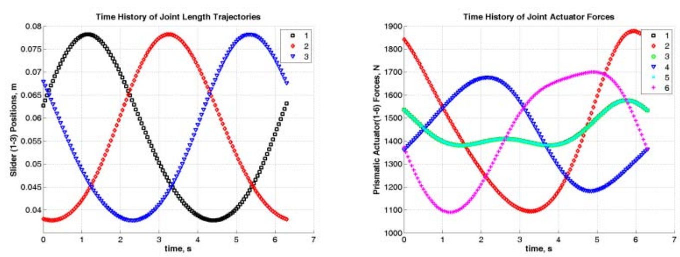

(A) (B)

Figure 13: ACTUATOR FORCE ESTIMATES FOR QUASI-STATIC SIMULATION FOR A CIRCULAR TRAJECTORY x = 0.08m, Y=0.01*cos(t) m, Z=0.01*sin(t) m (A) ACTUATOR FORCES (B) ACTUATOR DISPLACEMENTS

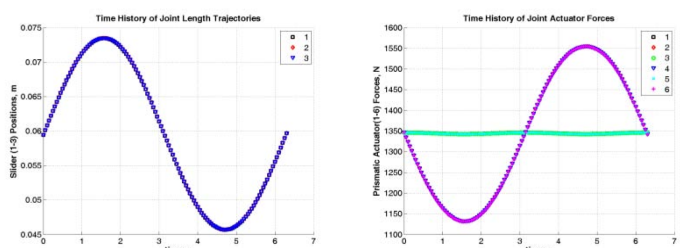

(A) (B)

Figure 14: ACTUATOR FORCE ESTIMATES FOR QUASI-STATIC SIMULATION FOR A YAW TRAJECTORY YAW = 10*sin(t) m, X=Y=Z=0, ZERO PITCH AND ROLL (A) ACTUATOR DISPLACEMENTS (B) ACTUATOR FORCES

ACKNOWLEDGMENTS

We gratefully acknowledge the support from the Research Foundation of State University of New York, National Science Foundation CAREER Award (IIS-0347653) and CNS-0751132.

REFERENCES

[1] Tsai, L.-W., Mar 2000, "Solving the Inverse Dynamics of Stewart- Gough Manipulator by the Principle of Virtual Work," Journal of Mechanical Design, 122(1), pp. 3-9.
[2] Kong, X., and Gosselin, C., 2007, *Type Synthesis of Parallel Mechanisms*, *Springer Tracts in Advanced Robotics* Springer Berlin / Heidelberg,
[3] Lou, Y., Liu, G., and Zexiang, L., 2007, "Randomized Optimal Design of Parallel Manipulators," IEEE Transactions on Automation Science and Engineering, 5(2), pp. 223-233.
[4] Bonev, I. A., Nov 2002, "Geometric Analysis of Parallel Mechanisms," Ph.D. thesis, Laval University, Canada, Quebec.
[5] Cherfia, A., Zaatri, A., and Giordano, M., 2007, "Kinematics Analysis of a Parallel Robot with a Passive Segment," Ingeniare - Revista Chilena de Ingeniería, 15(2), pp. 141-148.
[6] Tsai, L.-W., 1999, *Robot Analysis: The Mechanics of Serial and Parallel Manipulators*, A Wiley-Interscience Publication-John Wiley & Sons Inc.,
[7] Gosselin, C., and Angeles, J., 1990, "Singularity Analysis of Closed-Loop Kinematic Chains," IEEE Trans. on Robotics and Automation, 6(3), pp. 281-290.
[8] Joshi, S. A., and Tsai, L.-W., 2003, "The Kinematics of a Class of 3-DOF, 4-Legged Parallel Manipulators," Journal of Mechanical Design, 125(1), pp. 52-60.
[9] Merlet, J. P., and Gosselin, C. M., 1999, "Determination of 6D Workspaces of Gough-Type Parallel Manipulator and Comparison between Different Geometries," Mechanisms and Machine Theory, 26(1), pp. 77-99.
[10] Bonev, I., and Gosselin, C. M., September 10-13, 2000, "A Geometrical Algorithm for the Computation of the Constant Orientation Workspace of 6-R-U-S Parallel Manipulators," eds., Baltimore, MD, USA, pp. 505-514.
[11] Kecskemethy, A., Krupp, T., and Hiller, M., 1997, "Symbolic Processing of Multi-Loop Mechanism Dynamics Using Closed Form Kinematic Solutions," *Multibody System Dynamics*, 1(1), pp. 23-45.
[12] Durrbaum, A., Klier, W., and Hahn, H., 2002, "Comparison of Automatic and Symbolic Differentiation in Mathematical Modeling and Computer Simulation of Rigid Body Systems," *Multibody System Dynamics*, 7(4), pp. 331-355.
[13] Tancredi, L., Teillaud, M., and Devillers, O., 1996, "Symbolic Elimination for Parallel Manipulators," Technical Report No.2809, INRIA, Paris, France.
[14] Honegger, M., Codourey, A., and Burdet, E., "Adaptive Control of the Hexaglide, a 6 DOF Parallel Manipulator," Technical Report No. Institution of Robotics, ETH Zurich, Zurich, SWITZERLAND.
[15] http://www.parallemic.org/WhosWho/Companies/Profile002.html
[16] Merlet, J. P., and Gosselin, C. M., 1991, "New Architecture for a Six-Degree-of-Freedom Parallel Manipulator," Mechanism and Machine Theory, 26(1), pp. 363-385.
[17] Hopkins, B. R., and Williams, R. L., 2002, "Kinematics, Design and Control of 6-P S U Platform," Industrial Robot: An International Journal, 29(5), pp. 443-451.
[18] Kim, J.-P., and Ryu, J., 2002, "Inverse Kinematics and Dynamics of 6-DOF P-U-S Type Parallel Manipulators," KSME International Journal, 16(1), pp. 13-23.
[19] Rao, A. B. K., Saha, S. K., and Rao, P. V. M., 2006, "Dynamics Modeling of Hexaslides Using the Decoupled Natural Orthogonal Complement Matrices," Multibody Syst. Dynam., 15(2), pp. 159-180.
[20] Zhao, Y., and Gao, F., 2009, "Inverse Dynamics Analysis of 6-DOF out-Parallel Manipulator by Means of the Principle of Virtual Work " Robotica, 27(2), pp. 259-268.
[21] Narayanan, M. S., 2008, "Analysis of Parallel Manipulator Architectures for Use in Masticatory Studies," Ph.D. thesis, University at Buffalo (SUNY), Buffalo.